Applied and Environmental Microbiology, Oct. 2011, p. 6867–6877 Vol. 77, No. 19
0099-2240/11/$12.00 doi:10.1128/AEM.05272-11

Whole-Genome Sequencing and Phenotypic Analysis of *Bacillus subtilis* Mutants following Evolution under Conditions of Relaxed Selection for Sporulation[▽]

Christopher T. Brown,[1] Laura K. Fishwick,[1] Binna M. Chokshi,[1] Marissa A. Cuff,[1] Jay M. Jackson IV,[1] Travis Oglesby,[1] Alison T. Rioux,[1] Enrique Rodriguez,[1] Gregory S. Stupp,[1] Austin H. Trupp,[1] James S. Woollcombe-Clarke,[1] Tracy N. Wright,[1] William J. Zaragoza,[1] Jennifer C. Drew,[2] Eric W. Triplett,[1] and Wayne L. Nicholson[2]*

Department of Microbiology and Cell Science, University of Florida, Gainesville, Florida,[1] and Space Life Sciences Laboratory, Kennedy Space Center, Florida 32899[2]

Received 25 April 2011/Accepted 31 July 2011

Little is known about how genetic variation at the nucleotide level contributes to competitive fitness within species. During a 6,000-generation study of *Bacillus subtilis* evolved under relaxed selection for sporulation, a new strain, designated WN716, emerged with significantly different colony and cell morphologies; loss of sporulation, competence, acetoin production, and motility; multiple auxotrophies; and increased competitive fitness (H. Maughan and W. L. Nicholson, Appl. Environ. Microbiol. 77:4105–4118, 2011). The genome of WN716 was analyzed by OpGen optical mapping, whole-genome 454 pyrosequencing, and the CLC Genomics Workbench. No large chromosomal rearrangements were found; however, 34 single-nucleotide polymorphisms (SNPs) and +1 frameshifts were identified in WN716 that resulted in amino acid changes in coding sequences of annotated genes, and 11 SNPs were located in intergenic regions. Several classes of genes were affected, including biosynthetic pathways, sporulation, competence, and DNA repair. In several cases, attempts were made to link observed phenotypes of WN716 with the discovered mutations, with various degrees of success. For example, a +1 frameshift was identified at codon 13 of *sigW*, the product of which (SigW) controls a regulon of genes involved in resistance to bacteriocins and membrane-damaging antibiotics. Consistent with this finding, WN716 exhibited sensitivity to fosfomycin and to a bacteriocin produced by *B. subtilis* subsp. *spizizenii* and exhibited downregulation of SigW-dependent genes on a transcriptional microarray, consistent with WN716 carrying a knockout of *sigW*. The results suggest that propagation of *B. subtilis* for less than 2,000 generations in a nutrient-rich environment where sporulation is suppressed led to rapid initiation of genomic erosion.

The phenotypic plasticity of bacterial genomes enables bacteria to alter their gene expression in response to environmental stresses (18). A well-studied example of one such stress is the transition of *Bacillus subtilis* cells from exponential growth into the stationary phase upon nutrient limitation (49). Transition state genes in *B. subtilis* include those involved in such global responses as chemotaxis and motility; production of extracellular enzymes; production of, and resistance to, antibiotics; genetic competence; and initiation of sporulation (reviewed in reference 46). Sporulation itself is a complex developmental process requiring over 125 genes and taking about 6 to 8 h (7, 13, 48). Of these genes, about 21% are pleiotropic, i.e., also involved in housekeeping and other cellular processes (20). Thus, relaxing selective pressure for sporulation would be predicted to reduce the genetic interference from sporulation in pleiotropic genes and to allow greater potential for their variation in a population (14). Understanding how sporulating bacteria evolve under constant sporulation-repressing conditions can help us further elucidate how genes interact at the whole-organism level.

Laboratory evolution experiments have become important tools for exploring the underlying processes of evolution in microorganisms (6, 33). In previous communications, we have reported on evolution of five *B. subtilis* populations, WN624A through WN624E, that were cultivated for 6,000 generations in a sporulation-repressing, high-nutrient medium (R medium) (19–21). Populations 624A and 624C had reduced ability to sporulate, and three populations (624B, 624D, and 624E) lost this trait entirely (20). During the course of this evolution experiment, we noted a novel small-colony variant that appeared in, swept through, and became fixed in three out of the five evolving populations (624A, 624B, and 624E) (21). We showed that these small-colony variants had gained increased fitness in R medium and displayed a number of new phenotypic traits related to growth (a higher exponential growth rate and cell filamentation) and to the transition state (continued growth in postexponential phase; loss of motility, sporulation, and genetic competence; and altered fermentation profiles) (21).

* Corresponding author. Mailing address: Room 201-B, Space Life Sciences Laboratory, Building M6-1025/SLSL, Kennedy Space Center, FL 32899. Phone: (321) 861-3487. Fax: (321) 861-2925. E-mail: WLN@ufl.edu.

▽ Published ahead of print on 5 August 2011.

FIG. 1. Optical maps of ancestral strain WN624 (top), presweep strain WN715 (middle), and postsweep strain WN716 (bottom). Whole genomes of ancestral strain WN624 and evolved strains WN715 and WN716 were digested with NcoI, and optical maps of each strain were created by OpGen technology. The ~4-kb deletion detected in strain WN716 by optical mapping is indicated by the arrow. All other lines connecting maps are due to small inversions in palindromic regions generated by the mapping program (see Materials and Methods).

To better understand the genetic causes of increased fitness in the small-colony variants, the WN624A population was chosen for further studies. In this population, the small-colony variant appeared at generation 1,330 and completely swept through the culture in ~450 generations. Representative colonies from before (WN715) and after (WN716) the population sweep were isolated. The small-colony variant strain WN716 exhibited an unusual long, filamentous cell morphology that was distinct from the single rod-shaped cells characteristic of traditional *B. subtilis*, and the motility of WN716 was lost or greatly reduced. In competition experiments using R medium, even when strains WN715 and WN716 were inoculated at a 1,000:1 ratio, respectively, strain WN716 became the sole inhabitant and strain WN715 disappeared within ~40 generations (21).

Transcriptional microarrays were performed on RNA extracted from early-stationary-phase cells of WN715 versus WN716 to identify expression changes greater than 8-fold. The microarrays revealed genes involved in purine and pyrimidine biosynthesis and stress responses to be preferentially upregulated during early stationary phase in WN716. Genes for major autolysins, transport proteins, cytochromes, early sporulation functions, competence, antibiotic production, acetoin fermentation, and motility were preferentially downregulated in WN716 (21). These results suggested that the increased fitness of WN716 was not due to a single mutation but that a number of changes must have occurred during its evolution in order to result in its complex alteration of multiple phenotypic traits.

In this communication, we describe experiments undertaken with the purpose of identifying genomic changes leading to the observed phenotypes of evolved strain WN716, using two approaches. First, optical mapping was used to search for potential large-scale genetic changes (e.g., large deletions, insertions, or inversions). Second, whole-genome 454 pyrosequencing was used to identify small-scale changes (e.g., single-nucleotide polymorphisms [SNPs] or small insertions/deletions [indels]). Three strains from the 624A evolution experiment were subjected to analysis; ancestral strain WN624, presweep strain WN715, and postsweep strain WN716. Predicted phenotypes resulting from mutations identified in WN716 were tested.

MATERIALS AND METHODS

***B. subtilis* strains, media, and growth conditions.** The construction of the ancestral *B. subtilis* strain WN624 (*trpC2 amyE*::*spc*) and the evolution of strains WN715 (*trpC2 amyE*::*cat*) and WN716 (multiply auxotrophic; *amyE*::*spc*) have been described in detail previously (21). *B. subtilis* subsp. *spizizenii* strains NRRL B-23049^T and NRRL B14821 were generously donated by Mike Roberts, Team Qinetiq North America (31). The media used included R medium (21), LB medium (23), Schaeffer sporulation medium (SSM) (40), and Spizizen minimal medium (SMM) (47). When required, media were supplemented with the following antibiotics (final concentrations): chloramphenicol (5 μg/ml), spectinomycin (100 μg/ml), and rifampin (50 μg/ml). Fosfomycin and mitomycin C sensitivities were tested in liquid LB medium by 2-fold serial dilutions, giving final concentrations ranging from 0 to 800 μg/ml and 1 to 128 ng/ml, respectively, and cells were grown in 96-well microtiter plates at 37°C for 8 h before growth was measured. Where appropriate, SMM was supplemented with the following auxotrophic requirements (final concentrations): arginine (25 μg/ml), biotin (5 ng/ml), glutamate (25 μg/ml), histidine (25 μg/ml), and tryptophan (25 μg/ml). All growth was at 37°C with aeration. Testing of the resistance of strains WN624, WN715, and WN716 to the antibiotics produced by *B. subtilis* subsp. *spizizenii* was performed as described previously (2).

Optical mapping. Frozen cells of strains WN624, WN715, and WN716 were sent to OpGen (Madison, WI) for optical mapping. Each whole genome was digested with NcoI and scanned using their Argus optical-mapping technology. The optical maps of WN624, WN715, and WN716 were compared to each other and to an *in silico* map of the reference strain 168 to check for large-scale deletions, inversions, and translocations in their genomes. Palindromic regions were ignored or, often, misidentified by the program as inversions (Fig. 1), and changes smaller than 5 kbp were too small for the technology to resolve.

DNA isolation, 454 pyrosequencing, and mutation identification. DNA from *B. subtilis* strains was isolated as described previously (37). Whole-genome sequences of strains WN624, WN715, and WN716 were determined by 454 pyrosequencing. Sequencing libraries were prepared using the standard protocol and kit provided by 454 Life Sciences (Roche Diagnostics). NextGen (University of Florida) sequenced each genome on a 454 GS-FLXTM Standard 454 pyrosequencing platform. Each strain was then subjected to a genome-wide comparison to the reference genome, 168, using the CLC Genomics Workbench (CLC GW) alignment and annotation tools. Mutations (SNPs and indels) that were consistent among WN624, WN715, and WN716 (even if all three strains differed from the 168 reference sequence at the position in question) were discarded. We compiled a list of the remaining mutations that were the same in WN624 and WN715 but different in WN716 and verified each mutation by direct visual inspection of the sequence in CLC GW. Mutations that had fewer than 4 reads or less than 100% agreement were discarded.

Since homopolymeric regions are hot spots for misreads, mutations that occurred in these regions (*fliR*, *alsR*, *clpE*, and *lytD*), were verified by PCR amplification of the region and automated Sanger sequencing using an ABI 3130 DNA sequencer. Mutations that occurred within open reading frames of genes with known annotated functions (as predicted on NCBI for the reference genome) were further analyzed to determine their possible contributions to the phenotype of strain WN716. Mutations within intergenic regions were analyzed as follows.

TABLE 1. Genome assembly statistics[a]

Parameter	WN715			WN716		
	Count	Avg length	Total no. of bases	Count	Avg length	Total no. of bases
Reads	150,530	224.6	33,808,075.0	89,868	224.8	20,204,273.0
Matched	148,387	224.9	33,369,451.0	88,738	225.1	19,973,927.0
Not matched	2,143	204.7	438,624.0	1,130	203.9	230,346.0
Reference	1	4,215,606.0	4,215,606.0	1	4,215,606.0	4,215,606.0

[a] The genomes of strains WN715 and WN716 were sequenced using 454 pyrosequencing and aligned to the reference *B. subtilis* subsp. *subtilis* strain 168 genome (NCBI reference NC 000964.3).

The intergenic regions surrounding these mutations were identified using the Subtilist database (http://genolist.pasteur.fr/SubtiList/) (28, 29) and further examined using DBTBS (http://dbtbs.hgc.jp/; 44) to identify their locations within putative promoters, transcription factor binding sites, or transcriptional terminators. Mutations located within terminators were further analyzed using MFOLD (http://mfold.rna.albany.edu/; 54) to determine changes in stability possibly caused by the mutation in question.

RESULTS AND DISCUSSION

Optical maps. Long-term evolution of microbes under constant conditions often leads to irreversible loss of genomic material, a phenomenon known as genomic erosion (27). Previously, we had noted that a strain evolved from WN624 after ~6,000 generations of relaxed selective pressure for sporulation had sustained a deletion of ~10 kbp in the nonessential *ppsABCDE* operon (18). Therefore, in order to search for possible large-scale deletions or other gross alterations in genome architecture, an OpGen optical map was created for strains WN624, WN715, and WN716, as described previously (11). The genome maps were aligned using the Map Solver software supplied by OpGen. Comparison of the optical maps showed a single large deletion of about 4 kb in postsweep strainWN716 that was not present in ancestral strain WN624 or presweep strain WN715 (Fig. 1). However, subsequent 454 sequencing of the three strains revealed that this deletion was not present in strain WN716. Thus, this putative deletion was likely incorrectly identified due to the resolution limits of optical mapping (approximately 5 kb). Aside from the above observation, the overall optical maps of the three genomes aligned well with each other, indicating that the phenotypic changes observed in WN716 were not the result of major chromosomal rearrangements occurring before 1,800 generations (Fig. 1).

454 sequencing and alignment. To identify individual mutations that might account for the increased fitness of WN716, we used 454 pyrosequencing to sequence the genomes of strains WN715 and WN716. The resulting sequencing statistics are shown in Table 1. Before processing, our preliminary data revealed a total of 196 SNPs, 105 of which were verified according to our stringency qualifications as described in Materials and Methods. Of these 105 total SNPs, 11 were located in intergenic regions. Of the remaining 94 SNPs, located in coding regions, 27 were determined to result in silent mutations. Of the 67 remaining SNPs, 34 were located in genes of known function and 33 in genes of unknown function. Four mutations were found in homopolymeric regions, which are known to be susceptible to misreading by 454 pyrosequencing. In these cases, the regions in question were resequenced by Sanger sequencing, and the Sanger sequencing results agreed with the 454 data in each case (data not shown).

Of the 34 coding-sequence SNPs in genes of known function, we deduced 29 missense, 1 nonsense, and four +1 frameshift mutations (Table 2). These mutations were clustered in several categories of pathways, especially motility (*fliI*, *fliL*, *fliR*, and *motA*), sporulation (*cotX*, *spsI*, *minD*, *citB*, and *phrE*), stress response (*clpE* and *clpC*), biosynthesis of amino acids (*argH* and *carA*), cofactors (*bioF*), and antibiotics (*pksL*, *ppsE*, *srfAA*, and *sigW*) (Table 2). SNPs in some genes suspected to induce mutator phenotypes, including enzymes for DNA repair (*uvrB*) and recombination (*addA*), were also identified. Several mutations corresponded to genes previously found by microarray analysis to be up- or downregulated in WN716 compared to WN715 (21) (Table 3).

As can be seen in Table 2, most SNPs found within coding sequences were missense mutations, which might be predicted to affect the activity, stability, etc., of the target gene itself. However, some SNPs were either nonsense mutations or +1 frameshift mutations, which might be expected to also exert polar effects on downstream genes in the same operon. An exception to this supposition would be the monocistronic *gltP* and *clpE* genes (Table 2); +1 frameshifts in these two genes would not be expected to exert any polar effect. A nonsense mutation at codon 150 in *nagB* (Table 2) might affect the expression of the downstream *yvoA* gene, the function of which is unknown; however, microarray analysis detected only 0.58-fold less *yvoA* mRNA in WN716 than in WN715 (21). Downstream from the *sigW* cistron is located the *rsiW* cistron encoding an antisigma factor, RsiW, that regulates SigW activity (41). A +1 frameshift at codon 13 in *sigW* could result in loss of expression of the RsiW protein. However, the likely phenotype of a SigW$^-$ RsiW$^-$ double mutant would be identical to that of a SigW$^-$ single mutant, because (i) the target of RsiW regulation, SigW, is itself missing and (ii) expression of the *sigW-rsiW* operon is under SigW control (4). An interesting finding was a +1 frameshift located at codon 66 in the *fliR* gene, which is the 20th cistron in a large (31-gene) flagellar-chemotaxis (*fla-che*) operon (32). A frameshift in *fliR* might be expected to cause premature transcription termination, affecting the expression of the 11 downstream *fla-che* genes. It is interesting that the 30th cistron in the *fla-che* operon is *sigD*, which encodes the SigD sigma factor responsible for transcription of all flagellar, motility, and chemotaxis genes, including the *fla-che* operon (and *sigD*) itself. We previously noted that the mRNA levels of all motility genes, including the *fla-che* operon, were severely downregulated in strain WN716, but

TABLE 2. Identified mutations that altered the amino acid sequence encoded by genes of known function in strain WN716[a]

Gene or operon	Function	WN716 coverage at 100%	Amino acid change
Category 1. Cell envelope and cellular processes			
1.1 Cell wall			
dacC	Peptidoglycan biosynthesis, early stationary phase	4	G300S
lytD	Involved in cell separation, cell wall turnover, antibiotic-induced lysis	4[b]	S185L
wapA	Cell wall-associated protein precursor	8	P1578S
1.2 Transport/binding proteins and lipoproteins			
gltP	Glutamate uptake symport protein	4	+1 frameshift at codon 9
1.4 Membrane bioenergetics (electron transport chain, ATP synthase)			
qoxB	Cytochrome aa_3 quinol oxidase	4	A238V
1.5 Motility and chemotaxis:			
fliI	Flagellar ATP synthase	5	R338G
fliL	Required for flagellar formation	4	T54A
fliR	Required for flagellar formation	6[b]	+1 frameshift at codon 66
motA	Flagellar motor rotation	4	V221L
1.7 Cell division			
minD	Cell division inhibition (septum placement)	6	R33C
1.8 Sporulation			
cotX	Spore coat protein	6	A87V
spsI	Spore coat polysaccharide synthesis	5	R95H
phrE	Negative control of RapE activity	4	A37V
Category 2. Intermediary metabolism			
2.1 Metabolism of carbohydrates and related molecules			
2.1.1 Specific pathways			
nagB	*N*-Acetylglucosamine utilization	7	Nonsense at codon 150
2.1.2 Main glycolytic pathways			
pykA	Pyruvate kinase	5	E78G
tpiA	Triose phosphate isomerase	6	E249G
2.1.3 TCA[c] cycle			
citB	Aconitase	7	T616I
2.2 Metabolism of amino acids and related molecules			
argH	Arginine biosynthesis	6	A143V
carA	Arginine biosynthesis	4	A354V
hutU	Histidine utilization	4	V225A
2.5 Metabolism of coenzymes and prosthetic groups			
bioF	Biotin biosynthesis	4	A247S
Category 3. Information pathways			
3.2 DNA restriction/modification and repair			
uvrB	Excision of UV light-induced pyrimidine dimers in DNA	4	V498A
3.3 DNA recombination			
addA	Initiation stage of recombination	4	E522K
3.5 RNA synthesis			
3.5.1 Transcription initiation			
sigW	RNA polymerase ECF-type sigma factor	4	+1 frameshift at codon 13
3.5.2 Transcription regulation			
alsR	Regulation of the acetoin operon (*alsSD*)	3[b]	A21D
3.5.3 Transcription elongation			
rpoB	RNA polymerase	4	N269D
3.6 RNA modification			
miaA	Translation	8	S36N
Category 4. Other functions			
4.1 Adaptation to atypical conditions			
clpC	Class III stress response ATPase	10	S589P
clpE	ATP-dependent Clp protease-like (class III stress gene)	3[b]	+1 frameshift at codon 70
rsbS	Negative regulation of σ^B activity	7	L29S
4.3 Antibiotic production			
pksS	Polyketide synthase of type I	5	H2900R
ppsE	Plipastatin synthetase	5	Q1064R
srfAA	Surfactin production and competence	4	A782V
4.4 Phage-related function			
xkdT	PBSX prophage gene	5	A175V

[a] SNPs and indels were identified by aligning the whole genomes of WN624, WN715, and WN716 with the reference genome of *B. subtilis* 168 and identifying mutations present in WN716 and absent in the other strains. Silent mutations and mutations in genes of unknown function are not included in the table.

[b] Mutation was confirmed by Sanger sequencing.

[c] TCA, tricarboxylic acid.

TABLE 3. Mutations found between WN715 and WN716 that correlate with microarray data[a]

Gene	Function	Fold expression change in WN716	Amino acid change
pksS	Polyketide synthase type I	−8	H2900R
srfAA	Surfactin synthetase subunit 1	−17	A782V
fliI	Flagellum-specific ATP synthase	−12	R338G
fliR	Required for flagellum formation	−24	+1 frameshift at codon 66
lytD	*N*-Acetylglucosaminidase, major autolysin	−7	S185L
bioF	8-Amino-7-oxononanoate synthase	−4	A247S
alsR	Transcriptional regulator of *alsSD* operon	−122 (*alsS*), −87 (*alsD*)	A21D

[a] Microarray data from reference 21.

DNA sequencing failed to reveal any mutations in or around *sigD* (21). A polar effect of a frameshift in *fliR* could explain these observations.

Linking the WN716 phenotype with mutation in *sigW*. Several mutations identified in WN716 would be predicted to result in specific altered phenotypes. Where possible, these predictions were tested directly. For example, 454 sequencing identified a +1 frameshift mutation at codon 13 of the *sigW* gene, which encodes the alternative sigma factor σ^W (Table 2). The σ^W regulon in *B. subtilis* includes target genes involved in resistance to a number of bacteriocins and antibiotics produced by various microbes, including other *Bacillus* species (2–4). Therefore, loss of σ^W would be predicted to result in sensitivity of strain WN716 to antibiotics produced by other *Bacillus* spp. This prediction was tested by spotting cells of two strains of *B. subtilis* subsp. *spizizenii* onto lawns of *B. subtilis* strains WN624, WN715, and WN716 (Fig. 2). Strain WN716 was indeed more sensitive to the antibiotic(s) produced by the two *B. subtilis* subsp. *spizizenii* strains, as demonstrated by its larger zone of growth inhibition (Fig. 2). This observation is in excellent agreement with results obtained in a *sigW* knockout mutant (2). In addition, fosfomycin resistance, encoded by the *sigW*-dependent *fosB* gene (3), was tested by growing strains WN624, WN715, and WN716 in liquid LB medium containing various concentrations of fosfomycin and comparing their sensitivity profiles, presented here as the concentration of fosfomycin that inhibited the growth rate of cells by 50% (Fig. 3). Strain WN716 was observed to be dramatically more sensitive to fosfomycin than either ancestral strain WN624 or presweep strain WN715 (Fig. 3). Taken together, these results strongly suggest that the observed phenotypes are indeed caused by the *sigW* mutation in postsweep strain WN716.

Previously, we reported on the results of cDNA microarray experiments comparing the transcriptomes of WN715 and WN716 in early stationary-phase of growth in liquid R medium (21). The discovery of a frameshift mutation inactivating *sigW* in WN716 would be predicted to affect the transcription of genes belonging to the SigW regulon, which has been delineated previously (4). These observations prompted us to compare our microarray data with the microarray data published by Cao et al. (4), the results of which are presented in Table 4. We observed that several known members of the SigW regulon were downregulated in both microarrays, for example, the *yjoB*, *yknW*, *yoaF*, and *yvlA* genes and the *yqeZ-yqfAB*, *pspA-ydjGHI*, and *sppA-yteJ* operons, as well as the *sigW-rsiW* operon itself (Table 4). Thus, the microarray data support the prediction that WN716 has sustained a mutation inactivating *sigW*. However, it should be noted that comparison of the two sets of microarray data also revealed a number of discrepancies. For example, a set of genes (*abh*, *divIC*, *yfhKLM*, *yjbC-spx*, *yqjL*, *ywoA*, and *yxzE*) was observed to be downregulated in WN716 but not in the data of Cao et al. (4) (Table 4). Conversely, a number of genes (*pbpE-racX*, *ybfO*, *ydbS*, *yobJ*, *ysdB*, *ythPQ*, *yuaF*, *ywrE*, and *yxjJI*) were observed to be downregulated in

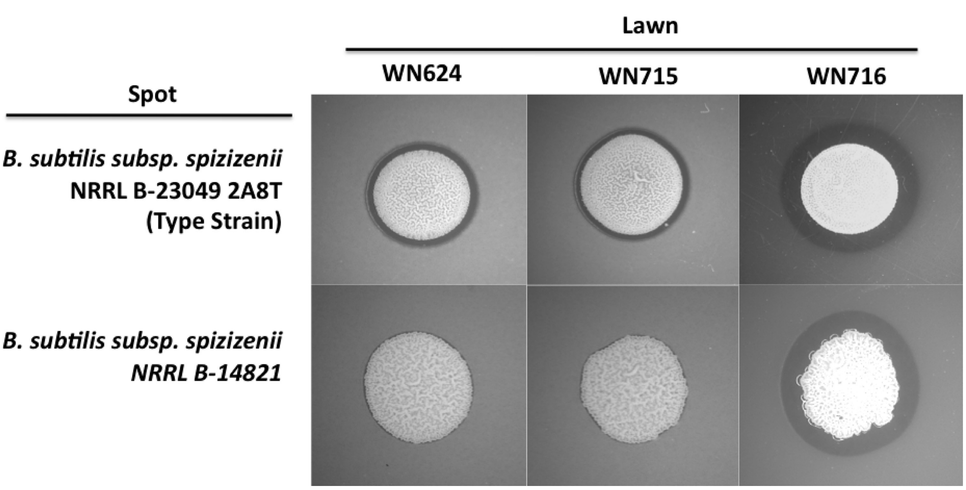

FIG. 2. Bacteriocin sensitivity assay. Lawns of strains WN624, WN715, and WN716 were plated onto LB medium, and aliquots of overnight liquid cultures of *B. subtilis* subsp. *spizizenii* were spotted onto the lawns. Zones of growth inhibition of the lawns can be seen as dark rings surrounding the colony spots.

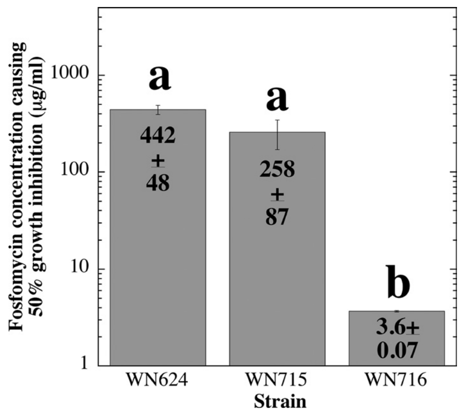

FIG. 3. Sensitivities of strains WN624, WN715, and WN716 to fosfomycin. The concentration of fosfomycin causing a 50% reduction in the growth rate was determined for each strain. The data are shown as averages ± standard deviations ($n = 3$). The lowercase letters above the bars denote significant differences (analysis of variance [ANOVA]; $P < 0.05$).

the data of Cao et al. (4) but not in WN716 (Table 4). Finally, a substantial number of known SigW-dependent genes were not significantly downregulated in either set of microarray data (Fig. 4). These apparent discrepancies are likely due to at least two factors. First, the two microarray experiments were performed on different pairs of strains, grown in different media, and harvested at different growth phases (4, 21). Second, the SigW regulon has been defined by a combination of several different approaches, including microarray analyses, bioinformatics techniques, and runoff macroarray (ROMA) analyses, none of which, applied by itself, was able to completely define the regulon (4). Thus, the lack of complete concordance between the two data sets is not surprising.

Mutations in *uvrB* and *addA*. Examination of SNPs in the WN716 genome identified missense mutations in the *uvrB* and *addA* genes (Table 2). The *uvrB* gene encodes the UvrB subunit of the UvrABC excinuclease involved in nucleotide excision repair of DNA damage, and *addA* encodes a component of the *B. subtilis* AddAB helicase-nuclease complex involved in general homologous recombination and in recombinational DNA repair (38, 39). Because mutants lacking UvrB or AddA are known to exhibit increased sensitivity to the DNA-damaging agent mitomycin C, we predicted that WN716 might also exhibit this phenotype. This prediction was tested by growing strains WN624, WN715, and WN716 in liquid LB medium containing various concentrations of mitomycin C and comparing their sensitivity profiles, presented here as the concentration of mitomycin C that inhibited the growth rate of cells by 50% (Fig. 4). Strain WN716 exhibited a modest but statistically significant 2.3-fold increase in mitomycin C sensitivity compared to ancestral strain WN624 (Fig. 4). However, strain WN715 also exhibited a 1.2-fold increase in mitomycin C sensitivity compared to the ancestor, so it is difficult to attribute mitomycin C sensitivity to mutations in *uvrB* and/or *addA* in this case. In any event, the increase in mitomycin C sensitivity observed was much less severe than would be expected of mutations completely inactivating either UvrB or AddA (15, 30).

Genome-sequencing analysis suggested that WN716 accumulated a substantial number of mutations within the first ~1,800 generations of evolution. Earlier data indicated that the bulk 624A population exhibited an ~50-fold increase in the rate of spontaneous mutation to rifampin resistance (Rif^r) during evolution, most of which had occurred within the first 2,000 generations, strongly suggesting that the evolving populations were accumulating cells with mutator phenotypes (19). Measurement of the frequency of mutation to Rif^r in pure cultures of strains WN624, WN715, and WN716 showed that the strains mutated to Rif^r at frequencies of 3.1×10^{-9}, 4.6×10^{-7}, and 4.7×10^{-6}, respectively. Thus, the spontaneous-mutation frequencies in evolved strains WN715 and WN716 had increased ~150-fold and ~1,500-fold, respectively, over that of the ancestral strain, WN624, in the course of less than 2,000 generations of evolution. Such high mutation frequencies strongly suggested that the evolved strains had sustained mutations in genes conferring a mutator phenotype, as has previously been observed in laboratory bacterial-evolution experiments (50). Interestingly, the *Escherichia coli* equivalents of the *uvrB* and *addA* gene products have both been implicated in stationary-phase hypermutagenesis (9). The AddA protein contains 6 helicase motifs important for activity (52), but the E522K mutation found in strain WN716 was not located in any of these regions (data not shown).

UvrB is an ATP-dependent DNA helicase (25), and examination of the deduced amino acid sequence of UvrB revealed that the V498A mutation in WN716 was located within highly conserved helicase motif V (Fig. 5A). In *E. coli* UvrB, nearby mutations in motif V (G502R and G509D/S) were shown to affect UvrB helicase activity and formation of the UvrABC preincision complex (25). In UvrB proteins from several bacterial species, amino acid 498 in motif V is often, but not always, valine (Fig. 5A) (51). Despite the fact that valine and alanine both carry small hydrophobic side groups, alanine-scanning mutagenesis experiments have revealed numerous V-to-A amino acid changes affecting protein activity (22). Taken together, the data suggest that the mutations in *uvrB* and/or *addA* might be partially responsible for the mutator phenotype observed in strain WN716. Genetic reconstruction experiments will test this notion directly.

Mutation in *alsR*. Strain WN716 was previously shown to be unable to produce the fermentation product acetoin in R medium, and microarray experiments showed that the *alsSD* (acetoin) operon was severely downregulated in WN716 (21). The *alsS* and *alsD* genes encode the enzymes α-acetolactate synthase and acetolactate decarboxylase, respectively (36). Divergently transcribed from *alsSD* is the *alsR* gene that encodes AlsR, a LysR family positive regulator of *alsSD* transcription; disruption of *alsR* was previously shown to result in severe downregulation of *alsSD* transcription and acetoin production (36). In this work, the WN716 genome sequence was found to contain a mutation in the *alsR* gene, which was predicted to result in the amino acid change A21D in the AlsR protein sequence (Tables 2 and 3). In AlsR, residue A21 is located within the helix-turn-helix (HTH) DNA-binding motif and is a highly conserved amino acid among all LysR family proteins (53) (Fig. 5B). Mutations in the HTH region of another LysR family protein, OxyR, have been shown to reduce or eliminate binding of the mutant OxyR proteins to their cognate DNA-

TABLE 4. SigW-dependent genes downregulated in the transcriptome of strain WN716 vs. that of WN715[a]

Gene or operon[b]	Annotated function[c]	Fold downregulation in WN716[d]
abh	Transcriptional regulator of transition state genes (AbrB-like)	7.0
divIC	Cell division initiation protein (septum formation)	5.4
fosB (*yndN*)	Cysteine-dependent fosfomycin resistance protein	<2.0 (<2.0)
pbpE	Penicillin-binding protein 4	<2.0 (7.7)
racX	Amino acid racemase	<2.0 (11)
pbpX	Penicillin-binding protein	<2.0
pspA (*ydjF*)	Alkaline shock-induced protein	2.1 (3.4)
ydjG	Conserved protein	3.7
ydjH	Conserved membrane protein	2.3
ydjI	Conserved protein	10.9
sigW	RNA polymerase ECF-type sigma factor	5.1 (10)
rsiW (*ybbM*)	Possible anti-SigW protein	9.4 (17)
sppA (*yteI*)	Signal peptide peptidase	2.2 (2.5)
yteJ	Conserved membrane protein	12.5 (2.2)
xpaC	5-Bromo-4-chloroindolyl phosphate hydrolysis protein	<2.0 (<2.0)
yaaN	Similar to toxic cation resistance protein	<2.0
ybfO	Similar to erythromycin esterase	<2.0 (3.2)
yceC	Similar to tellurium resistance protein	2.5 (<2.0)
yceD	Similar to tellurium resistance protein	<2.0
yceE	Similar to tellurium resistance protein	<2.0
yceF	Similar to tellurium resistance protein; probable transporter	<2.0
yceG	Conserved protein	<2.0
yceH	Similar to toxic anion resistance protein	<2.0
ydbS	Conserved membrane protein	<2.0 (3.2)
ydbT	Conserved membrane protein	2.1 (3.0)
yeaA	Conserved protein	<2.0
ydjP	Similar to chloroperoxidase	<2.0
ydjO	Function unknown and unique	<2.0
yfhK	Similar to *B. subtilis ywsB*	6.1
yfhL	Function unknown and unique	2.5 (<2.0)
yfhM	Similar to epoxide hydrolase	3.0
yjbC	Conserved protein	3.8 (<2.0)
yjbD (*spx*)	Glutaredoxin family; disruption bypasses the ClpXP requirement for ComK expression	4.8
yjoB	Similar to FtsH	4.3 (25)
yknW	Conserved membrane protein	4.4 (2.2)
yknX	Conserved protein	<2.0
yknY	Probable ABC transport system ATP-binding protein	2.6
yknZ	Probable ABC transport system permease protein	<2.0 (2.8)
yoaF	Function unknown and unique	2.0 (2.0)
yoaG	Similar to prophage protein	− (2.4)
yobJ	Function unknown and unique	<2.0 (4.0)
yozO	Conserved protein	<2.0 (<2.0)
yqeZ	Conserved membrane protein	− (9.5)
yqfA	Conserved protein	15.1 (6.7)
yqfB	Function unknown and unique	8.1 (5.6)
yqjL	Function unknown and unique	6.6
yrhH	Similar to methyltransferase	<2.0 (<2.0)
ysdB	Conserved protein	<2.0 (10)
ythP	Similar to ABC transport system ATP-binding protein	<2.0 (31)
ythQ	Function unknown and unique	<2.0 (16)
yuaF	Function unknown and unique	<2.0 (89)
yuaG	Conserved protein	<2.0
yuaI	Probable acetyltransferase	2.5 (11)
yvlA	Function unknown and unique	3.9 (2.7)
yvlB	Conserved protein	2.8
yvlC	Conserved protein	<2.0 (2.1)
yvlD	Conserved membrane protein	<2.0 (2.3)
ywaC	Similar to GTP-pyrophosphokinase	<2.0 (<2.0)
ywbL	Putative transporter	<2.0
ywbM	Conserved protein	<2.0
ywbN	Conserved protein	<2.0 (<2.0)
ywnJ	Function unknown and unique	<2.0
ywoA	Bacitracin resistance protein	3.7 (<2.0)
ywrE	Conserved membrane protein	<2.0 (11)
yxjJ	Conserved protein	<2.0
yxjI	Function unknown and unique	<2.0 (12)
yxzE	Function unknown and unique	2.5 (<2.0)

[a] Microarray data were obtained from early-stationary-phase cultures of strains WN715 and WN716 grown in liquid R medium (21).
[b] SigW-dependent genes compiled from the DBTBS database (http://dbtbs.hgc.jp/; 44).
[c] Annotated functions taken from the *Bacillus subtilis* genome database BSORF (http://bacillus.genome.ad.jp/).
[d] Microarray data for WN715 vs. WN716 are derived from reference 21. Microarray data for the wild type vs. the *sigW* mutant (in parentheses) are taken from reference 4. −, not included on micrarray.

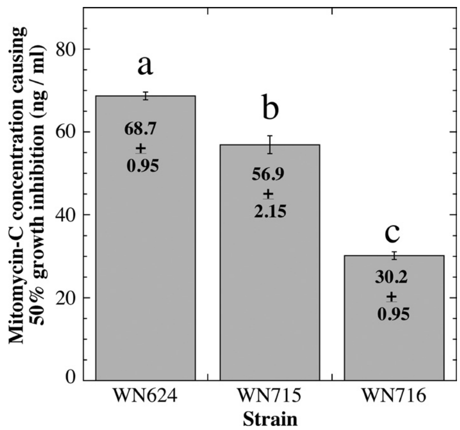

FIG. 4. Sensitivities of strains WN624, WN715, and WN716 to mitomycin C. The concentration of mitomycin C causing a 50% reduction in the growth rate was determined for each strain. The data are shown as averages ± standard deviations ($n = 3$). The lowercase letters above the bars denote significant differences (ANOVA; $P < 0.05$).

binding sites (16). Collectively these observations suggest that the A21D mutation in WN716 AlsR may be directly responsible for downregulation of *alsSD* transcription and loss of acetoin production. Experiments to test this notion are currently in progress.

Mutations in biosynthetic pathways. Sequence analysis also uncovered a number of missense mutations in several biosynthetic (*argH*, *bioF*, *carA*, *citB*, and *hutU*) or glutamate-transport (*gltP*) genes, inactivation of which would be predicted to result in nutritional auxotrophies, in addition to the *trpC* marker present in all strains used here (Table 2). Note that mutation

A

```
                                 Helicase motif V
         ::: *:**:: ::**:::** **:  :*:**********:***
UvrB 460 IKVNYLHSEIKTLERIEIIRDLRLGKYDVLVGINLLREGLDIP 512
                                     ↓  ↓      ↓
                              (WN716)A  R      D
                                               S
```

B

```
                         D(WN716)
               10        20↑       30        40
               |         | |       |         |
AlsR MELRHLQYFIAVAEELHFGKAARRLNMTQPPLSQQIKQLEEEVGVT
     * :* * *::*:**  ** :**  ::::** ** **: **:*:**
OxyR MNIRDLEYLVALAEHRHFRRAADSCHVSQPTLSGQIRKLEDELGVM
        ↓                          ↓↓↓
        C                          MFN
     --HHHHHHHHHHHH---HHHHHHHH---HHHHHHHHHHHHHHH---
             α1           α2           α3
```

FIG. 5. (A) Deduced amino acid sequence of the *B. subtilis* UvrB protein. Helicase motif V (12) is underlined and labeled. Mutations altering UvrB helicase and incision activity (G502R, G509D, and G509S) (25) are indicated by downward arrows. Valine 498 is boxed, and the V498A mutation in strain WN716 is indicated. (B) Deduced N-terminal amino acid sequences of AlsR and OxyR. The underlined amino acids are highly conserved among LysR family proteins (53). Alanine 21 in AlsR is boxed, and the A21D mutation in AlsR is indicated by the upward arrow. The downward arrows denote mutations in the OxyR HTH region leading to decreased DNA binding (16). The bottom line indicates the position and extent of alpha-helices (α1, α2, and α3) in the LysR HTH region (53). In both panels, the asterisks and colons denote identical and conserved amino acids. See the text for details.

TABLE 5. Growth of *B. subtilis* strains on supplemented Spizizen minimal medium[a]

Strain	Growth on Spizizen minimal medium supplemented with:					
	BGHT	AGHT	ABHT	ABGT	ABGH	ABGHT
WN624	+	+	+	+	−	+
WN715	+	+	+	+	−	+
WN716	−	−	−	−	−	−

[a] A, arginine; B, biotin; G, glutamate; H, histidine; T, tryptophan; +, growth; −, no growth.

in the aconitase gene *citB* also leads to sporulation deficiency, as well as glutamate auxotrophy (5) (Table 2). Growth of strains WN624, WN715, and WN716 on SMM plates containing various combinations of arginine, biotin, glutamate, histidine, and tryptophan showed that both strains WN624 and WN715 had retained the original *trpC2* marker and had not gained additional auxotrophy for other nutrients (Table 5). In contrast, growth of WN716 on SMM supplemented with all five nutrients (tryptophan, biotin, histidine, arginine, and glutamate) failed to rescue its auxotrophic phenotype (Table 5), indicating that strain WN716 carried at least one other auxotrophy in addition to those tested. Therefore, in this case, genomic sequence analysis fell short of identifying all mutations responsible for the multiply auxotrophic phenotype of strain WN716.

SNPs located in intergenic regions. It was reasoned that SNPs occurring in intergenic regions could affect gene expression through alterations in regulatory sequences, such as promoters, binding sites for transcription factors, or transcription terminators. Thus, an attempt was made to locate the 11 intergenic SNPs found in strain WN716 within known or putative regulatory sites using *B. subtilis* databases. Of the 11 SNPs originally identified as located in intergenic regions, no discernible regulatory feature could be identified in 5 cases; furthermore, one SNP was actually located in the last codon of the *pcp* gene, resulting in an H-to-L amino acid change (Table 6). The remaining 5 SNPs were located in putative regulatory sites. One SNP was located in the previously characterized Zur box C2, located upstream from the *yciC* gene encoding a putative zinc transport protein (10); however, the SNP did not change *yciC* expression in WN716 on the microarray (Table 6). A second SNP was located in a putative AraR-binding site located between the divergently transcribed *nudF* and *yqkF* genes, encoding an ADP-ribose pyrophosphatase and a putative oxidoreductase, respectively. This SNP did not result in a dramatic change in *nudR* or *yqkF* mRNA levels on the microarray (Table 6), and indeed, it is difficult to envision how or why *nudR* or *yqkF* would be subject to AraR regulation, because the AraR repressor specifically regulates genes involved in arabinose and hemicellulose metabolism (35). A third SNP was located within a putative Fur box located between *recO*, encoding a recombination/DNA repair protein, and *era*, encoding a GTP-binding protein essential for cell growth; again, no evidence for altered mRNA levels in WN716 was detected by microarray, and the *recO* and *era* genes were not identified as part of the Fur regulon (1). A fourth SNP was located in a putative MntR-binding site between the *hutG* (formiminoglutamase) and *hutM* (histidine permease) genes; these genes

TABLE 6. SNPs found in intergenic regions in WN716[a]

SNP	Position	Intergenic region	Comment	Expression in WN716 (microarray)[b]	Server[c] used or reference
T to G	119844	*rplA-rplJ*	No feature found	−2.8 (*rplA*) −2.6 (*rplJ*)	S, D, M
A to T	211093	*ybcI-ybcL*	No feature found	−1.1 (*ybcI*) −0.7 (*ybcL*)	S, D
A to T	286973	*pcp-ybcU*	Mutation in last codon of *pcp*; CAC(H) to CTC(L)	−0.1 (*pcp*) − (*ybcU*)	S
G to A	365358	*yciB-yciC*	Mutation in Zur box C2 upstream from *yciC*	− (*yciB*) −0.4 (*yciC*)	S, D 10
G to A	688754	*yeaC-yeaD*	No feature found	−0.1 (*yeaC*) −4.7 (*yeaD*)	S, D
T to C	953843	*ygzA-ygaJ*	No feature found	−2.2 (*ygzA*) −0.9 (*ygaZ*)	S, D
T to C	2458407	*nudF-yqkF*	Divergent genes; SNP located in a putative AraR-binding site	−1.8 (*nudF*) −0.6 (*yqkF*)	S, D
A to G	2609075	*recO-era*	SNP located within a putative Fur box	−1.7 (*recO*) −0.6 (*era*)	S, D
G to A	2838039	*csbX-yrbE*	No feature found	+0.48 (*csbX*) −0.6 (*yrbE*)	S, D
T to C	4046515	*hutG-hutM*	SNP located within a putative MntR-binding site	−0.4 (*hutG*) −0.6 (*hutM*)	S, D
T to C	4194778	*yyaJ-maa*	Convergent genes. SNP located in stem of putative *maa* transcription terminator; reduces ΔG from −17 to −13 kcal/mol	−2.7 (*yyaJ*) −2.3 (*mma*)	S, D, M

[a] SNPs located within intergenic regions were first located in Subtilist; the intergenic regions were then imported into DBTBS and searched for putative promoters or binding sites, for accessory transcription factors, and for transcriptional terminators. If the SNP was found in a terminator stem-loop, MFOLD was used to calculate the potential change in stability.
[b] Microarray data are from reference 21. −, gene was not spotted on the microarray.
[c] Abbreviations for internet servers: S, Subtilist (http://genolist.pasteur.fr/SubtiList/); D, DBTBS (http://dbtbs.hgc.jp/); M, MFOLD (http://mfold.rna.albany.edu/).

have not been identified as part of the MntR regulon (26), nor were their mRNA levels altered in WN716 on microarrays. The fifth SNP was located between the convergent *yyaJ* and *maa* genes encoding a putative transporter and a probable maltose *o*-acetyltransferase (Table 6). The last SNP was located in the stem region of the putative transcriptional terminator for *maa* and was predicted to lower the base-pairing stability of the stem from −17 to −13 kcal/mol. In this case, a slight (~2-fold) decrease in the mRNA levels was observed in strain WN716 on the microarrays (Table 6). Taken together, the 11 SNPs detected in intergenic regions were not found to correlate with significant gene expression changes or with known phenotypic changes in strain WN716.

Linking genomic changes with fitness. Continued evolution under constant environmental conditions can lead to massive loss of genetic material, a phenomenon often referred to as genomic erosion (27). In support of this notion, we previously observed that cells from populations 624A and 624B that had been propagated for 6,000 generations in R medium had sustained a >9.7-kb deletion in the *ppsABCDE* operon encoding biosynthesis of the nonessential antibiotic plipastatin (18). In this study, optical mapping revealed that there had been no discernible large-scale genomic changes in either WN715 or WN716 in the ~1,800 generations since their descent from WN624, suggesting that the source of WN716's increased competitive fitness likely was small mutations, including SNPs and/or indels, rather than large deletions, translocations, or inversions in the genome. The optical-mapping data supported our strategy of using 454 pyrosequencing to discover small mutations for the source of WN716's enhanced fitness.

Strain WN716 cells grow in R medium as long nonmotile filaments, and previous microarray experiments demonstrated downregulation of at least 45 genes, including all the flagellar operons and several *lyt* genes encoding autolysins (21). Because flagellar operons and *lyt* genes belong to the *sigD* regulon (42), their downregulation might have been due to mutation in the *sigD* gene itself. However, no mutation in the *sigD* coding sequence was identified in WN716, either by 454 pyrosequencing (this study) or by directed Sanger sequencing (21). Interestingly, 454 pyrosequencing did identify numerous mutations in *sigD*-dependent genes, such as the *lytD*, *fliI*, *fliL*, *fliR*, and *motA* genes (Table 2), and as discussed above, a frameshift mutation in *fliR* could possibly exert a polar effect on the expression of the downstream *sigD* gene itself. Furthermore, mutations were identified in genes belonging to several biosynthetic pathways in strain WN716 (Table 5). One explanation for these two observations could be that, because there is little or no selective pressure for maintaining functional motility or biosynthetic pathways in WN716 evolving under constant, nutrient-rich conditions, these genes are rapidly accumulating mutations, i.e., are in the process of becoming pseudogenes (17, 24).

In contrast, sequence analysis did identify a +1 frameshift mutation that would potentially inactivate the *sigW* gene encoding σ^W, which is known to control a regulon of antibiotic and bacteriocin resistance genes (2–4). Phenotypic characterization of strain WN716 (Fig. 3 and 4) and comparison of microarray data obtained for WN716 and an authentic *sigW* mutant (Table 4) strongly suggests that strain WN716 indeed appears to be defective in σ^W function.

Loss of either (or both) *sigD*- and *sigW*-directed functions would be selectively advantageous for strain WN716, because maintenance of motility, chemotaxis, and resistance to multiple antibiotics is energetically costly and confers no selective advantage during shake flask propagation in a nutrient-rich environment in the absence of nutrient concentration gradients or niche competitors. In support of this notion, large-scale flux analyses demonstrated that the metabolic efficiency of *B. subtilis* cells was actually improved in *sigD* or *sigW* knockout mutants (8). Thus, knockout of the *sigD* and/or *sigW* regulon would be predicted to result in a higher growth rate (i.e., enhanced fitness) of WN716 in R medium.

Strain WN716 was previously observed to have substantially lost both sporulation ability and competence for genetic transformation; furthermore, microarray analysis resulted in the identification of several genes encoding early sporulation and competence functions, transcription of which appeared to be severely downregulated (21). Although the exact cause of the sporulation deficiency of strain WN716 remains unclear at this time, mutations were identified in several candidate genes affecting sporulation. In addition to genes directly involved in spore formation (*cotX* and *spsI*, encoding a spore coat protein and a polysaccharide, respectively), we found mutations in genes involved in both competence and sporulation initiation. For example, a point mutation in *phrE* may affect sporulation and/or competence by limiting the ability of PhrE to assert negative control over the RapE phosphatase (34). A polarity-changing point mutation in *minD* could affect sporulation by disrupting septum placement during sporulation (43); however, microscopic examination of strain WN716 cells failed to reveal minicell production (data not shown). Finally, a mutation in the *citB* gene, encoding the Krebs cycle enzyme aconitase, was identified by 454 pyrosequencing (Table 2). Mutations inactivating aconitase are known to block sporulation at its earliest stage (5, 45). It seems reasonable to speculate that each of these mutations, either individually or in combination, could contribute to strain WN716's lack of genetic competence and its inability to sporulate. Future efforts will concentrate on obtaining direct experimental evidence for this supposition.

Despite the failure of optical mapping to reveal gross genomic changes, 454 pyrosequencing identified several small genomic changes that had occurred during the evolution of *B. subtilis* cells under relaxed selective pressure for sporulation. In particular, mutations were identified in the genome of WN716 that allowed testing of specific predicted phenotypes; in one case (mutation in *sigW*), the predicted phenotype was confirmed, while in other cases (motility, competence for transformation, sporulation, and acetoin biosynthesis), mutations were identified in genes which potentially led to the observed phenotype but which remain to be experimentally tested. In the case of auxotrophy, the loss of prototrophy was previously observed to be a consequence of evolution in nutrient-rich R medium in all evolving *B. subtilis* populations tested (19). Examination of population 624A had revealed that at generation 1,000 (before strain WN716 swept the culture), essentially 100% of the cells were prototrophic (aside from tryptophan auxotrophy conferred by the *trpC2* marker present in the ancestral strain), but by generation 2,000 (after the sweep), prototrophy had decreased dramatically to only 0.1% of the cells in the population (19). In the present study, whole-genome sequencing of strain WN716 revealed five mutations in four biosynthetic pathway genes, but an additional mutation(s) responsible for its multiply auxotrophic phenotype clearly remains to be discovered.

In conclusion, whole-genome sequencing revealed that strain WN716 had sustained a number of mutations that, individually or collectively, could contribute to its selective advantage in R medium. An important future step is to identify which mutated genes are responsible for WN716's selective advantage by producing targeted mutations inactivating specific genes and testing the resulting mutants in pairwise competition experiments (21, 33). These experiments are currently in progress.

ACKNOWLEDGMENTS

We thank Bill Farmerie at the UF ICBR NextGen sequencing group for his help with the 454 pyrosequencing and SNP/indel detection, John Helmann for helpful discussions, Mike Roberts for generous donation of *B. subtilis* subsp. *spizizenii* strains, and the four anonymous reviewers for insightful comments.

Much of the work described in this communication was performed as part of an undergraduate course, MCB4934 "Bacterial Genome Sequencing," under the direction of J.C.D., E.W.T., and W.L.N.

This work was supported in part by grants from the NASA Astrobiology, Exobiology, and Evolutionary Biology program (NNX08AO15G) to W.L.N. and from the Course, Curriculum and Laboratory program at the National Science Foundation (0920151) to J.C.D. and E.W.T.

REFERENCES

1. **Baichoo, N., T. Wang, R. Ye, and J. D. Helmann.** 2002. Global analysis of the *Bacillus subtilis* Fur regulon and the iron starvation stimulon. Mol. Microbiol. **45:**1613–1629.
2. **Butcher, B. G., and J. D. Helmann.** 2006. Identification of *Bacillus subtilis* σ^W-dependent genes that provide intrinsic resistance to antimicrobial compounds produced by *Bacilli*. Mol. Microbiol. **60:**765–782.
3. **Cao, M., B. A. Bernat, Z. Wang, R. N. Armstrong, and J. D. Helmann.** 2001. FosB, a cysteine-dependent fosfomycin resistance protein under the control of σ^W, an extracytoplasmic-function σ factor in *Bacillus subtilis*. J. Bacteriol. **183:**2380–2383.
4. **Cao, M., et al.** 2002. Defining the *Bacillus subtilis* σ^W regulon: a comparative analysis of promoter consensus search, run-off transcription/macroarray analysis (ROMA), and transcriptional profiling approaches. J. Mol. Biol. **316:**443–457.
5. **Craig, J. E., M. J. Ford, D. C. Blaydon, and A. L. Sonenshein.** 1997. A null mutation in the *Bacillus subtilis* aconitase gene causes a block in Spo0A-phosphate-dependent gene expression. J. Bacteriol. **179:**7351–7359.
6. **Elena, S. F., and R. E. Lenski.** 2003. Evolution experiments with microorganisms: the dynamics and genetic basis of adaptation. Nat. Rev. Genet. **4:**457–469.

7. **Errington, J.** 1993. *Bacillus subtilis* sporulation: regulation of gene expression and control of morphogenesis. Microbiol. Mol. Biol. Rev. **57:**1–33.
8. **Fischer, E., and U. Sauer.** 2005. Large-scale *in vivo* flux analysis shows rigidity and suboptimal performance of *Bacillus subtilis* metabolism. Nat. Genet. **37:**636–640.
9. **Foster, P. L.** 2007. Stress-induced mutagenesis in bacteria. Crit. Rev. Biochem. Mol. Biol. **42:**373–397.
10. **Gabriel, S. E., F. Miyagi, A. Gaballa, and J. D. Helmann.** 2008. Regulation of the *Bacillus subtilis yciC* gene and insights into the DNA-binding specificity of the zinc-sensing metalloregulator Zur. J. Bacteriol. **190:**3482–3488.
11. **Giongo, A., H. L. Tyler, U. N. Zipperer, and E. W. Triplett.** 2010. Two genome sequences of the same bacterial strain, *Gluconacetobacter diazotrophicus* PAl 5, suggest a new standard in genome sequence submission. Stand. Genomic Sci. **2:**309–317.
12. **Gorbalenya, A. E., E. Koonin, A. P. Donchenko, and V. M. Blinov.** 1989. Two related superfamilies of putative helicases involved in replication, recombination, repair, and expression of DNA and RNA. Nucleic Acids Res. **17:** 4713–4730.
13. **Graumann, P. (ed.).** 2007. *Bacillus*: cellular and molecular biology. Caister Academic Press, Wymondham, United Kingdom.
14. **Hansen, T.** 2003. Is modularity necessary for evolvability? Remarks on the relationship between pleiotropy and evolvability. Biosystems **69:**83–94.
15. **Kooistra, J., B. Vosman, and G. Venema.** 1988. Cloning and characterization of a *Bacillus subtilis* transcription unit involved in ATP-dependent DNase synthesis. J. Bacteriol. **170:**4791–4797.
16. **Kullik, I., J. Stevens, M. B. Toledano, and G. Storz.** 1995. Mutational analysis of the redox-sensitive transcriptional regulator OxyR: regions important for DNA binding and multimerization. J. Bacteriol. **177:**1285–1291.
17. **Lawrence, J. G., R. W. Hendrix, and S. Casjens.** 2001. Where are the pseudogenes in bacterial genomes? Trends Microbiol. **9:**535–540.
18. **Maughan, H., C. W. Birky, and W. L. Nicholson.** 2009. Transcriptome divergence and the loss of plasticity in *Bacillus subtilis* after 6,000 generations of evolution under relaxed selection for sporulation. J. Bacteriol. **191:**428–433.
19. **Maughan, H., et al.** 2006. The population genetics of phenotypic deterioration in experimental populations of *Bacillus subtilis*. Evolution **60:**686–695.
20. **Maughan, H., J. Masel, C. W. Birky, and W. L. Nicholson.** 2007. The roles of mutation accumulation and selection in loss of sporulation in experimental populations of *Bacillus subtilis*. Genetics **177:**937–948.
21. **Maughan, H., and W. L. Nicholson.** 2011. Increased fitness and the alteration of metabolic pathways during *Bacillus subtilis* laboratory evolution. Appl. Environ. Microbiol. **77:**4105–4118.
22. **Mercante, J., K. Suzuki, X. Cheng, P. Babitzke, and T. Romeo.** 2006. Comprehensive alanine-scanning mutagenesis of *Escherichia coli* CsrA defines two subdomains of critical functional importance. J. Biol. Chem. **281:**31832–31842.
23. **Miller, J. H.** 1972. Experiments in molecular genetics. Cold Spring Harbor Laboratory Press, Cold Spring Harbor, NY.
24. **Mira, A., H. Ochman, and N. A. Moran.** 2001. Deletional bias and the evolution of bacterial genomes. Trends Genet. **17:**589–596.
25. **Moolenaar, G. F., R. Visse, M. Ortiz-Buysse, N. Goosen, and P. van de Putte.** 1994. Helicase motifs V and VI of the *Escherichia coli* UvrB protein of the UvrABC endonuclease are essential for the formation of the preincision complex. J. Mol. Biol. **240:**294–307.
26. **Moore, C. M., and J. D. Helmann.** 2005. Metal ion homeostasis in *Bacillus subtilis*. Curr. Opin. Microbiol. **8:**188–195.
27. **Moran, N. A., H. J. McLaughlin, and R. Sorek.** 2009. The dynamics and time scale of ongoing genomic erosion in symbiotic bacteria. Science **323:**379–382.
28. **Moszer, I.** 1998. The complete genome of *Bacillus subtilis*: from sequence annotation to data management and analysis. FEBS Lett. **430:**28–36.
29. **Moszer, I., P. Glaser, and A. Danchin.** 1995. SubtiList: a relational database for the *Bacillus subtilis* genome. Microbiology **141:**261–268.
30. **Munakata, N.** 1977. Mapping of the genes controlling excision repair of pyrimidine photoproducts in *Bacillus subtilis*. Mol. Gen. Genet. **156:**49–54.
31. **Nakamura, L. K., M. S. Roberts, and F. M. Cohan.** 1999. Relationship of *Bacillus subtilis* clades associated with strains 168 and W23: a proposal for *Bacillus subtilis* subsp. *subtilis* subsp. nov. and *Bacillus subtilis* subsp. *spizizenii* subsp. nov. Int. J. Syst. Bacteriol. **49:**1211–1215.
32. **Ordal, G. W., L. M. Márquez-Magaña, and M. J. Chamberlin.** 1992. Motility and chemotaxis in *Bacillus subtilis*, p. 765–784. *In* A. Sonenshein, J. A. Hoch, and R. Losick (ed.), *Bacillus subtilis* and other gram-positive bacteria: biochemistry, physiology, and molecular genetics. ASM Press, Washington, DC.
33. **Palsson, B.** 2011. Adaptive laboratory evolution. Microbe **6:**69–74.
34. **Perego, M., and J. A. Hoch.** 2002. Two-component systems, phosphorelays, and regulation of their activities by phosphatases, p. 473–481. *In* A. L. Sonenshein, J. A. Hoch, and R. Losick (ed.). *Bacillus subtilis* and its closest relatives: from genes to cells. ASM Press, Washington, DC.
35. **Raposo, M. P., J. M. Inácio, L. J. Mota, and I. de Sá-Nogueira.** 2004. Transcriptional regulation of genes encoding arabinan-degrading enzymes in *Bacillus subtilis*. J. Bacteriol. **186:**1287–1296.
36. **Renna, M. C., N. Najimudin, L. R. Winik, and S. A. Zahler.** 1993. Regulation of the *Bacillus subtilis alsS, alsD,* and *alsR* genes involved in post-exponential-phase production of acetoin. J. Bacteriol. **175:**3863–3875.
37. **Roesch, L. W. F., et al.** 2009. Influence of fecal sample storage on bacterial community diversity. Open Microbiol. J. **3:**40–46.
38. **Sanchez, H., B. Carrasco, S. Ayora, and J. C. Alonso.** 2007. Homologous recombination in low dC+dG Gram-positive bacteria. Top. Curr. Genet. **17:**27–52.
39. **Sanchez, H., B. Carrasco, S. Ayora, and J. C. Alonso.** 2007. Dynamics of DNA double-strand break repair in *Bacillus subtilis*, p. 43–66. *In* P. Graumann (ed.), *Bacillus*: cellular and molecular biology. Caister Academic Press, Wymondham, United Kingdom.
40. **Schaeffer, P., J. Millet, and J.-P. Aubert.** 1965. Catabolic repression of bacterial sporulation. Proc. Natl. Acad. Sci. U. S. A. **54:**704–711.
41. **Schöbel, S., S. Zellmeier, W. Schumann, and T. Wiegert.** 2004. The *Bacillus subtilis* σ^W anti-sigma factor RsiW is degraded by intramembrane proteolysis through YluC. Mol. Microbiol. **52:**1091–1105.
42. **Serizawa, M., et al.** 2004. Systematic analysis of SigD-regulated genes in *Bacillus subtilis* by DNA microarray and Northern blotting analyses. Gene **329:**125–136.
43. **Sharp, M. D., and K. Pogliano.** 2002. MinCD-dependent regulation of the polarity of SpoIIIE assembly and DNA transfer. EMBO J. **21:**6267–6274.
44. **Sierro, N., Y. Makita, M. J. L. de Hoon, and K. Nakai.** 2008. DBTBS: a database of transcriptional regulation in *Bacillus subtilis* containing upstream intergenic conservation information. Nucleic Acids Res. **36:**D93–D96.
45. **Sonenshein, A. L.** 2002. The Krebs citric acid cycle, p. 151–162. *In* A. L. Sonenshein, J. A. Hoch, and R. Losick (ed.), *Bacillus subtilis* and its closest relatives: from genes to cells. ASM Press, Washington, DC.
46. **Sonenshein, A. L., J. A. Hoch, and R. Losick (ed.).** 2002. *Bacillus subtilis* and its closest relatives: from genes to cells. ASM Press, Washington, DC.
47. **Spizizen, J.** 1958. Transformation of biochemically deficient strains of *Bacillus subtilis* by deoxyribonucleate. Proc. Natl. Acad. Sci. U. S. A. **44:**1072–1078.
48. **Stragier, P., and R. Losick.** 1996. Molecular genetics of sporulation in *Bacillus subtilis*. Annu. Rev. Genet. **30:**297–341.
49. **Strauch, M. A., and J. A. Hoch.** 1993. Transition-state regulators: Sentinels of *Bacillus subtilis* post-exponential gene expression. Mol. Microbiol. **7:**337–342.
50. **Tanaka, M. M., C. T. Bergstrom, and B. R. Levin.** 2003. The evolution of mutator genes in bacterial populations: the roles of environmental change and timing. Genetics **164:**843–854.
51. **Theis, K., P. J. Chen, M. Skorvaga, B. Van Houten, and C. Kisker.** 1999. Crystal structure of UvrB, a DNA helicase adapted for excision repair. EMBO J. **18:**6899–6907.
52. **Yeeles, J. T. P., E. J. Gwynn, M. R. Webb, and M. S. Dillingham.** 2011. The AddAB helicase-nuclease catalyses rapid and processive DNA unwinding using a single Superfamily 1A motor domain. Nucleic Acids Res. **39:**2271–2285.
53. **Zaim, J., and A. M. Kierzek.** 2003. The structure of full-length LysR-type transcriptional regulators: modeling of the full-length OxyR transcription factor dimer. Nucleic Acids Res. **31:**1444–1454.
54. **Zuker, M.** 2003. Mfold web server for nucleic acid folding and hybridization prediction. Nucleic Acids Res. **31:**3406–3415.